Cranial irradiation compromises neuronal architecture in the hippocampus

Vipan Kumar Parihar and Charles L. Limoli[1]

Department of Radiation Oncology, University of California, Irvine, CA 92697-2695

Edited* by James E. Cleaver, University of California San Francisco, San Francisco, CA, and approved June 18, 2013 (received for review April 18, 2013)

Cranial irradiation is used routinely for the treatment of nearly all brain tumors, but may lead to progressive and debilitating impairments of cognitive function. Changes in synaptic plasticity underlie many neurodegenerative conditions that correlate to specific structural alterations in neurons that are believed to be morphologic determinants of learning and memory. To determine whether changes in dendritic architecture might underlie the neurocognitive sequelae found after irradiation, we investigated the impact of cranial irradiation (1 and 10 Gy) on a range of micromorphometric parameters in mice 10 and 30 d following exposure. Our data revealed significant reductions in dendritic complexity, where dendritic branching, length, and area were routinely reduced (>50%) in a dose-dependent manner. At these same doses and times we found significant reductions in the number (20–35%) and density (40–70%) of dendritic spines on hippocampal neurons of the dentate gyrus. Interestingly, immature filopodia showed the greatest sensitivity to irradiation compared with more mature spine morphologies, with reductions of 43% and 73% found 30 d after 1 and 10 Gy, respectively. Analysis of granule-cell neurons spanning the subfields of the dentate gyrus revealed significant reductions in synaptophysin expression at presynaptic sites in the dentate hilus, and significant increases in postsynaptic density protein (PSD-95) were found along dendrites in the granule cell and molecular layers. These findings are unique in demonstrating dose-responsive changes in dendritic complexity, synaptic protein levels, spine density and morphology, alterations induced in hippocampal neurons by irradiation that persist for at least 1 mo, and that resemble similar types of changes found in many neurodegenerative conditions.

radiation-induced cognitive dysfunction | radiation injury | structural plasticity

Radiotherapy is used routinely to control the growth of CNS malignancies and remains a frontline treatment for nearly all types of pediatric and adult brain tumors. The capability of cranial irradiation to forestall the advance of brain cancer has improved survival, but has also increased the number of patients living longer with severe neurocognitive sequelae (1–4). Significant evidence has now linked radiation exposure of the CNS to the eventual onset of cognitive dysfunction (5). The affected cognitive domains are diverse, and include disruptions in learning, memory, processing speed, attention, and executive function (3). Although there is growing awareness of the negative impact of radiation-induced cognitive dysfunction, the precise mechanisms underlying the causes and persistence of this serious side effect, as well as the contribution of patient-to-patient differences, such as disease status, genetic background, and treatment strategy, remain unknown.

The CNS is relatively radioresistant, able to withstand significant dose (typically up to 50–60 Gy) before incurring overt morphologic injury and normal tissue toxicity to the parenchymal and stromal compartments of the brain (6, 7). Based on experimental data in rodent models (8–10), these doses are likely to far exceed those typically required for the onset of radiation-induced cognitive dysfunction, which can manifest at much lower total doses (i.e., ≤10 Gy) than those used clinically (6, 11). More radiosensitive populations of neural stem and progenitor cells do exist in the neurogenic regions of the brain, and radiation-induced depletion of these cells in the hippocampal dentate gyrus has been linked to spatial-temporal learning and memory deficits (9, 10, 12). Although a wealth of evidence has conclusively shown that irradiation leads to impaired neurogenesis that likely contributes to cognitive impairment, much less is known concerning the impact of irradiation on more mature neurons. Given the relatively small percentage of neurogenic cells that functionally integrate into the hippocampal circuitry (13), the adverse effects of irradiation on cognition are likely to include alterations to more mature neuronal subsets that collectively impact the structural and synaptic plasticity of the irradiated CNS.

Much of the rationale for analyzing the impact of irradiation on neuronal morphometry is based on extensive studies linking changes in dendritic and spine morphology to a wide range of neurodegenerative conditions. As the principal site of synaptic contact, dendrites control the number and pattern of synapses received by neurons. Correspondingly, dendritic morphology dictates many aspects of neuronal function, including action potential propagation and information processing. Alterations in the geometry and branching pattern of the dendritic tree can be profound, and are often accompanied by severe cognitive disorders that impact learning and memory (14–16). Reductions in dendritic complexity are observed in many brain disorders, such as epilepsy (17), recurrent depressive illness (18), Alzheimer's disease (19), and Huntington disease (20), and dendritic abnormalities exhibit strong correlations with mental retardation found in Down syndrome (21), Rett syndrome (22), and Fragile-X syndromes (20). Thus, it is not surprising that the functional integrity of the CNS is directly related to neuronal morphology, as the proper growth and arborization of dendrites are crucial for cognitive health (15).

The interconnectivity of neural networks is fundamental to the proper functioning of the CNS. The formation and establishment of such a network requires precisely regulated growth and branching of dendritic arbors and spines, activity-dependent synaptogenesis, and simultaneous pruning and remodeling of dendritic structure. Neurotransmission is critically dependent upon the formation of specific types of dendritic spines localized to the postsynaptic membrane of many types of neurons. These specialized structures function as integrative units in the synaptic circuitry. A pronounced decrease in dendritic spines occurs in several neurological conditions, especially those associated with cognitive impairment (23). For example, spines are morphologically abnormal in certain forms of mental retardation and decreases in spine number and atypical morphology occur during normal aging in rodents and humans (24–27). Furthermore, reductions in dendritic spines accompany temporal lobe epilepsy, Huntington disease, and acquired immunodeficiency syndrome-related dementia (23). Spines have been proposed to mediate

Author contributions: V.K.P. and C.L.L. designed research; V.K.P. performed research; V.K.P. and C.L.L. analyzed data; and V.K.P. and C.L.L. wrote the paper.

The authors declare no conflict of interest.

*This Direct Submission article had a prearranged editor.

[1]To whom correspondence should be addressed. E-mail: climoli@uci.edu.

This article contains supporting information online at www.pnas.org/lookup/suppl/doi:10.1073/pnas.1307301110/-/DCSupplemental.

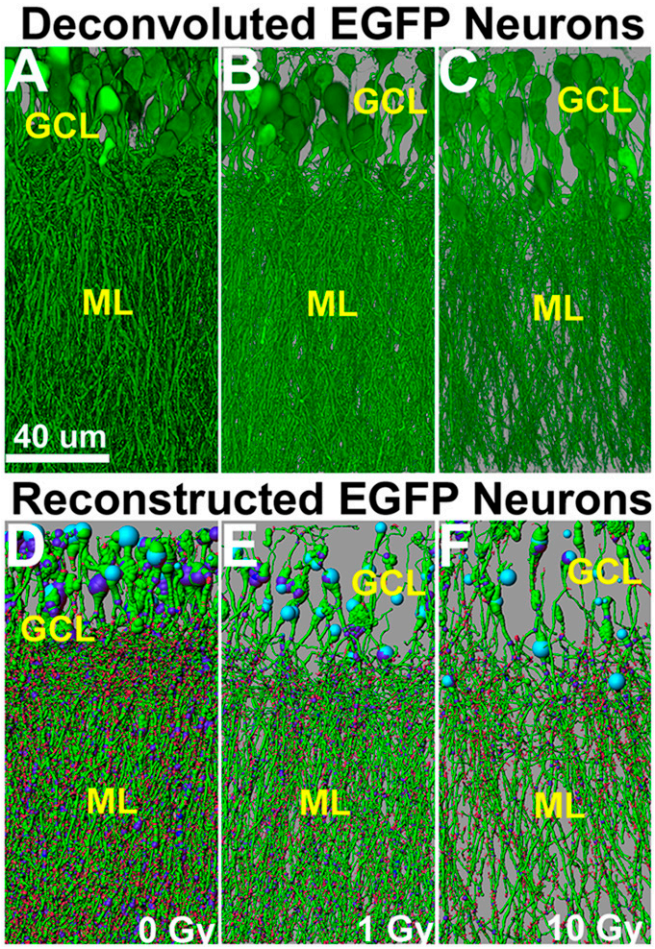

Fig. 1. Reduced dendritic complexity of GCL neurons 30 d after irradiation. (*A–C*) Examples of deconvoluted EGFP$^+$ GCL neurons showing dendrites orientated vertically and traversing the ML. (*D–F*) Deconvoluted 3D reconstructed images of *A–C*, respectively, with dendrites containing spines projecting into the ML (sky blue, cell body; green, dendrites; blue, branch points; red, spines).

both chemical and structural synaptic plasticity, and changes in their number clearly track with synaptic density, which in turn positively correlate with cognition (28).

The foregoing indicates that changes in dendritic complexity, spine morphology, and synaptic density are critical determinants for learning and memory and underlie many neurodegenerative sequelae. Based on the capability of irradiation to elicit many overlapping neurocognitive complications, we sought to determine if and how exposure to radiation might elicit acute and chronic alterations to the anatomical structure of neurons using a transgenic mouse model that expresses enhanced green fluorescent protein (EGFP) in certain subsets of neurons. Here we describe our findings regarding the impact of irradiation on neuronal micromorphometric parameters, including dendritic anatomy, spine morphology, and synaptic density.

Results

Radiation-Induced Reductions in Dendritic Complexity. The inherent fluorescence of the EGFP-expressing neurons in our selected transgenic mouse model provide for a detailed analysis of neuronal micromorphometry. Animals subjected to low- (1 Gy) or high- (10 Gy) dose γ-irradiation were analyzed over time for changes in dendritic complexity. Neurons analyzed in the granule cell layer (GCL) of the hippocampus exhibit significant dose-responsive reductions in dendritic complexity 10 d (Fig. S1 and Table S1) or 30 d (Fig. 1 and Table S2) following exposure. Radiation-induced reductions in dendritic complexity are readily apparent in deconvoluted (Fig. 1 *A–C*) and reconstructed (Fig. 1 *D–F*) images. Reconstructed images (nine total) were used to quantify changes in the number of dendritic branches, branch points, length, and area compared with unirradiated controls 10 or 30 d after irradiation (Fig. 2). Although reductions of these morphometric endpoints trended lower 10 d after 1 Gy, each endpoint was reduced significantly after the higher 10 Gy dose (Fig. 2, *Upper*). Compared with controls, mean values of dendritic branches (48%, $P < 0.01$), branch points (47%, $P < 0.01$), total length (54%, $P < 0.05$), and total area (37%, $P < 0.05$), were markedly lower after 10 Gy (Table S1).

Quantification of these same endpoints 30 d following the same doses confirmed both similar and persistent radiation-induced changes in morphometric parameters (Fig. 2 and Table S2). In contrast, however, to the earlier 10-d time point, the lower dose of 1 Gy led to significant reductions in all morphometric endpoints analyzed, clearly visible on both deconvoluted (Fig. 1 *A–C*) and reconstructed (Fig. 1 *D–F*) images derived from tissues 30 d postirradiation. At the lower dose, reduced numbers of dendritic branches (51%, $P < 0.01$), branch points (50%, $P < 0.05$), total length (51%, $P < 0.05$), and total area (53%, $P < 0.05$) were found compared with controls (Fig. 2, *Lower*, and Table S2). Dendritic complexity was compromised further at the higher 10-Gy dose when analyzed 30 d after exposure (Fig. 2, *Lower*). At this dose, reduced numbers of dendritic branches (51%, $P < 0.01$), branch points (59%, $P < 0.01$), total length (63%, $P < 0.01$), and total area (65%, $P < 0.01$) were found compared with controls (Table S2). These data demonstrate clearly that irradiation leads to dose-dependent and persistent reductions in the dendritic complexity of hippocampal neurons.

Radiation-Induced Reductions in Dendritic Spines. The presence of brightly fluorescent GCL neurons greatly facilitates the quantification of dendritic spines and spine morphology following irradiation. Analysis of several dendritic spine parameters 10 or 30 d following exposure revealed significant and persistent dose-responsive changes (Fig. 3 and Tables S3–S5). At 10 d post-irradiation, the higher dose (10 Gy) reduced significantly the

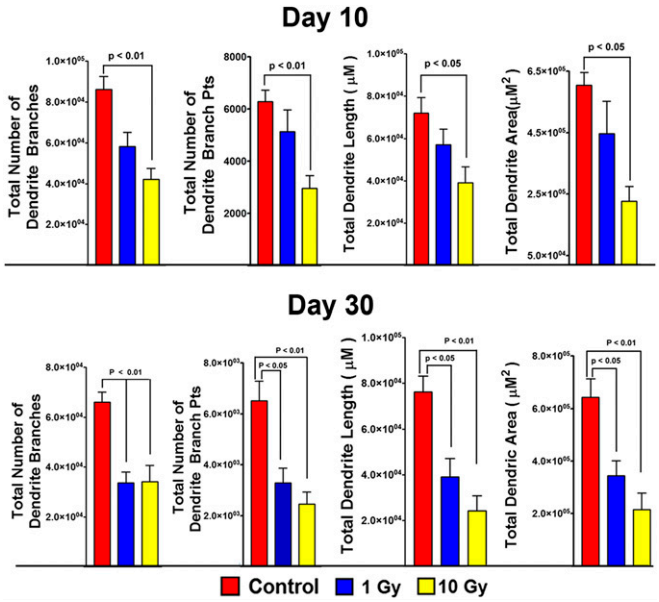

Fig. 2. Quantification of morphometric parameters 10 and 30 d after irradiation. Quantified morphometric parameters of dendritic complexity including dendrite branching, branch points, dendrite length, and dendrite area 10 d (*Upper*) and 30 d (*Lower*) after irradiation.

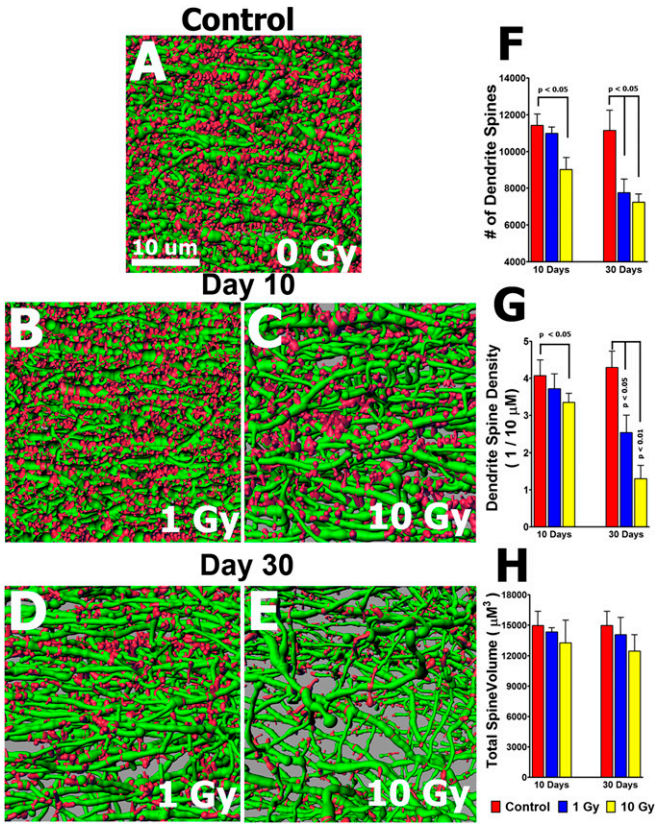

Fig. 3. Radiation-induced reductions in dendrite spine density. (*A–E*) Representative images 3D reconstructed dendritic segments (green) containing spines (red). (*F–H*) Quantified dendritic spine parameters including spine number (*F*), spine density (*G*), and spine volume (*H*) along GCL neurons 10 or 30 d after irradiation.

number of spines by 22% compared with controls ($P < 0.05$) (Fig. 3 *C* and *F*). However, at 30 d postirradiation, both 1 and 10 Gy significantly reduced the number of dendritic spines by 30% ($P < 0.05$) (Fig. 3 *D* and *F*) and 35% ($P < 0.05$) (Fig. 3 *E* and *F*), respectively. Related measurements of spine density confirmed similar trends at 10 d postirradiation, with 1 Gy causing minimal change, whereas 10 Gy reduced spine density by 18% compared with controls ($P < 0.05$) (Fig. 3 *D* and *G*). These changes were increased significantly at the 30-d time point, where spine density was reduced by 41% ($P < 0.05$) and 69% ($P < 0.01$) after 1 and 10 Gy, respectively (Fig. 3 *D*, *E*, and *G*). Spine volumes were comparable in irradiated and control mice at both radiation doses and time points analyzed (Fig. 3*H*).

Immature Filopodia Exhibit Relative Sensitivity to Irradiation. To analyze further potential differences in the susceptibility of morphologically distinct spines to irradiation, distinct subclasses of spines were categorized and quantified at 10 and 30 d following exposure (Fig. 4 and Tables S6 and S7). Reconstructed dendritic segments were scrutinized for changes in specific subclasses of spines at different time after irradiation, as shown in representative images (Fig. 4 *A–C*). Dendritic spines were classified as either filopodia, long, mushroom, or stubby based on rigorous morphometric criteria (*Methods* and Fig. 4*D*). Evident from the data were that long, mushroom, and stubby spines along GCL neurons were relatively resistant to radiation, because the yields of these more mature spine morphologies were not found to change significantly compared with unirradiated controls. Further analysis of the number of spines comprising each category revealed that irradiation had the largest impact on filopodia (Fig. 4 *E* and *F*). The yield of filopodia was significantly reduced by 40% ($P < 0.05$) 10 d after the higher dose of 10 Gy (Fig. 4*E*). By day 30 postirradiation, both 1- and 10-Gy doses reduced the yield of filopodia by 43% ($P < 0.05$) and 73% ($P < 0.01$), respectively, compared with controls (Fig. 4*F*). These data clearly show that spines of defined morphology exhibit differential susceptibility to irradiation.

Radiation-Induced Changes in Synaptic Proteins: Up-Regulation of Postsynaptic Density Protein (PSD-95) in the Dentate Gyrus. To analyze further the consequences of irradiation on hippocampal neurons, immunohistochemistry was undertaken to measure the levels of selected of synaptic proteins. The postsynaptic density protein (PSD-95) plays a major role in regulating synaptic plasticity and can be visualized as discrete immunostained puncta that can be deconvoluted and quantified. Neurons analyzed in the GCL and molecular layer (ML) showed significant increases in the level of PSD-95 expression after each radiation dose compared with controls 10 and 30 d postirradiation (Fig. 5 and Table S8). The yield of PSD-95 puncta in the GCL and ML after 1 Gy increased significantly by 71% ($P < 0.05$) and 120% ($P < 0.01$) compared with controls 10 and 30 d postirradiation, respectively (Fig. 5 *B–D*). At the higher dose of 10 Gy, the number of PSD-95 puncta in the same hippocampal subfields increased significantly by 170% ($P < 0.01$) compared with controls at either postirradiation time (Fig. 5 *B*, *E*, and *F*). Data indicate clearly the capability of irradiation to elevate the level of PSD-95 puncta over an extended period.

Radiation-Induced Changes in Synaptic Proteins: Down-Regulation of the Presynaptic Protein Synaptophysin in the Dentate Hilus. The effects of irradiation were also analyzed in the dentate hilus (DH), a hippocampal subfield enriched in presynaptic terminals. For these studies the presynaptic marker synaptophysin was

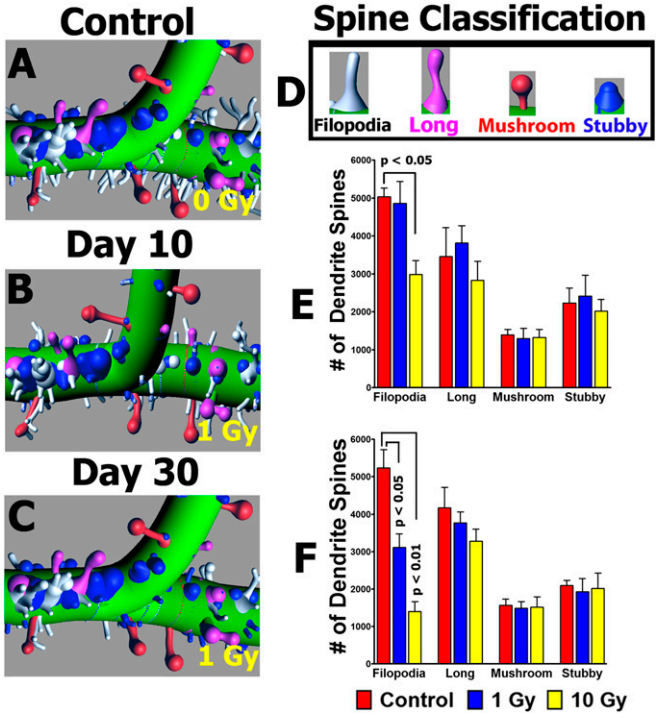

Fig. 4. Radiation-induced changes in the number of morphologically distinct spines. Reconstructed dendritic segments showing the radiation-induced reductions in filopodia (white, *A–C*) along with other spine types after irradiation, using the color-coded classification shown (*D*). (*E* and *F*) Quantified spine types including immature filopodia along with more mature long, mushroom, and stubby morphologies 10 (*E*) and 30 (*F*) d following irradiation.

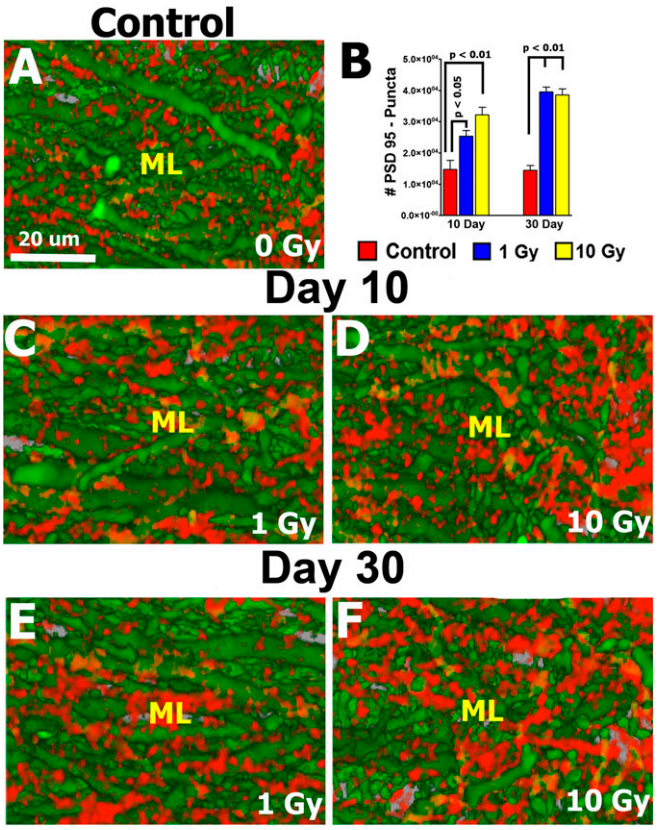

Fig. 5. Up-regulation of PSD-95 expression following irradiation. Deconvoluted images show that irradiation leads to increased expression of PSD-95 puncta (red) in GCL neurons of the ML at both 10 (*C* and *D*) and 30 (*E* and *F*) d after irradiation compared with controls (*A*). (*B*) Quantified PSD-95 puncta at 10 and 30 d after exposure to 1 and 10 Gy.

analyzed by immunohistochemistry 10 and 30 d following irradiation by confocal microscopy (Fig. 6 and Table S9). In unirradiated controls, synaptophysin puncta were more frequent, with individual clusters containing greater numbers of puncta compared with irradiated samples. Reduced staining was evident by day 10 following irradiation and became more extensive and uniform throughout the dentate gyrus by day 30. At the earlier 10-d time, synaptophysin expression was reduced significantly in the DH by 40% ($P < 0.05$) and 55% ($P < 0.01$) after 1 and 10 Gy, respectively, compared with controls (Fig. 6 *B–D*). At the latter 30-d time, the expression of synaptophysin was still reduced significantly, lower by 32% ($P < 0.05$) and 70% ($P < 0.01$) after 1 and 10 Gy, respectively, compared with controls (Fig. 6 *B*, *E*, and *F*). Data show that irradiation can induce a dose-responsive and persistent reduction in the level of synaptophysin.

Discussion

Micromorphomertric analysis provides insight into the types of structural changes induced by irradiation in the CNS. The use of transgenic mice expressing EGFP in specific subsets of neurons greatly facilitates quantitative measurements, thereby obviating the need for more traditional and time-consuming approaches dependent on dye-loading or Golgi-staining of neurons (29). With this system, we have identified neurons within specific hippocampal subfields that satisfy strict morphologic criteria and systematically applied neuron-tracing and spine-analysis algorithms to rigorously characterize the long-term structural plasticity induced by acute radiation exposure. With this approach we have identified significant and persistent radiation-induced reductions in dendritic complexity and spine density along with marked changes in the levels of pre- and postsynaptic proteins in the irradiated hippocampus. These changes are likely contributory, if not causal, to many of the multifaceted neurocognitive complications experienced by patients subjected to cranial irradiation for the treatment of brain cancer.

To elucidate radiation-induced changes in neuronal anatomy, measurements of total dendritic length, numbers of dendritic intersections, nodes, and endings along with spine number, density, volume, and morphology were quantified. Noteworthy among our findings were the significant dose-responsive reductions in dendritic complexity that persisted 1 mo following acute irradiation (Figs. 1 and 2). Although the impact of irradiation on dendritic structure was pronounced, reduced numbers of GCL neurons (particularly at the 10-Gy dose) may have contributed to the reductions in dendritic complexity found after irradiation. Reduced dendritic arborization was accompanied by significantly lower numbers of dendritic spines and spine density, with relatively moderate changes in the spine volume (Fig. 3). More detailed analyses of spine morphologies revealed that irradiation had a relatively mild impact on more mature spines (stubby, mushroom, long) (Fig. 4). Interestingly, irradiation had a significant impact on immature filopodia, leading to marked dose-responsive reductions in the population of these newly forming spines at all times analyzed (Fig. 4). As structural elements that mediate both chemical and structural synaptic plasticity, spines regulate the connectivity of the CNS (30). Although their morphology varies widely, likely reflecting functional diversity, changes in spine density positively correlate with cognitive performance (31). The capability of dendritic spines to rapidly respond to transmembrane signals, including those associated with behavior, hormonal status,

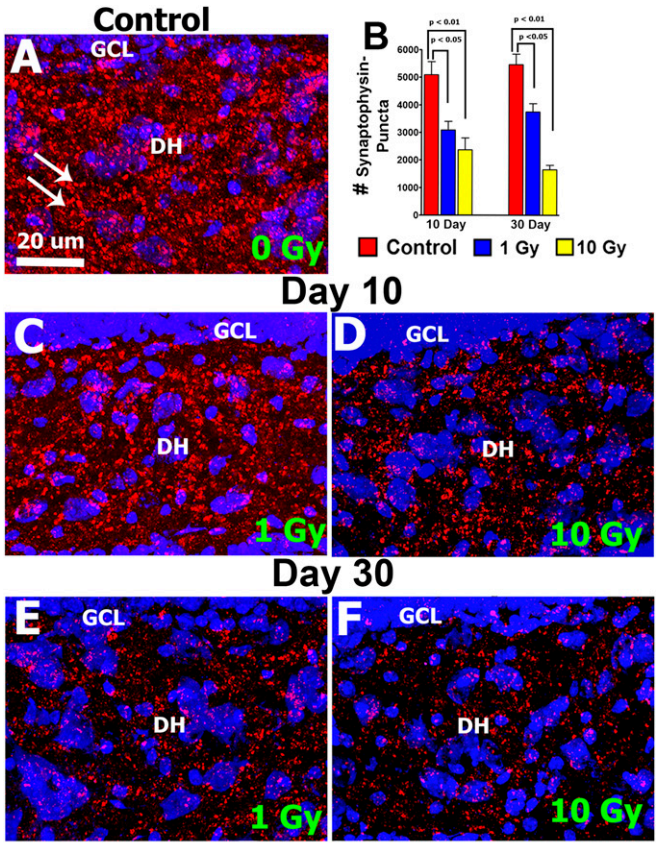

Fig. 6. Down-regulation of the presynaptic marker synaptophysin following irradiation. Representative images of synaptophysin expression show reduced expression in the DH at both 10 (*C* and *D*) and 30 (*E* and *F*) d after irradiation compared with controls (*A*). (*B*) Quantified synaptophysin staining at 10 and 30 d after exposure to 1 and 10 Gy.

and synaptic activity and various forms of stress, indicate their critical role in learning and memory (32, 33). The fact that radiation exposure leads to reduced spine density and, in particular, inhibits the formation of immature filopodia, is consistent with the adverse neurocognitive sequlae documented in brain cancer survivors subjected to cranial radiotherapy (1, 34). The persistence of these structural changes coincides with the protracted recovery of the irradiated CNS, and is again consistent with the progressive and irreversible nature of radiation-induced cognitive dysfunction (11, 35).

Our findings provide unique evidence for the marked structural changes induced by irradiation in hippocampal neurons. A recent study has reported irradiation to reduce dendritic spine density, an effect that could be ameliorated by manipulating the oxidative microenvironment (36). The capability of irradiation to induce an acute and persistent oxidative stress in vitro and in vivo (11) suggest changes in the microenvironmental redox state may play a role in the regulation of spine density and morphology. Another report focused on the analysis of dendritic spines in Golgi-stained neurons in the dentate gyrus and CA1 subfields of the hippocampus also found irradiation (10 Gy) to reduce spine density, but to a much lesser extent than that reported here (37). Relatively small but significant changes in mature spine morphologies were also found, an effect not detected in the present study. Although inherent differences in the anatomical characterization between Golgi-stained versus fluorescent neurons exist, the analysis of dendritic spines in the present study involved over 65,000–100,000 individual spines per animal (or 260,000–400,000 total spines per cohort), thereby demonstrating the statistical power of our approach.

Various mechanisms operate to modulate synaptic plasticity, including changes in receptor numbers, neurotransmitter release, and the regional localization of synaptic sites. Radiation-induced alterations in dendritic branching patterns, spine density, and morphology likely disrupt some, if not all, of the foregoing processes to compromise synaptic transmission in the irradiated brain. Quantification of PSD-95 puncta in the irradiated hippocampus revealed a significant and persistent increase in the expression of PSD-95 in the GCL and ML subfields of the dentate gyrus compared with controls. Previous studies have shown that PSD-95 contributes to the processes of dendrite development, spine formation, and spine maturation (38). Furthermore, the involvement of PSD-95 in dendritic spine maturation and clustering of synaptic signaling proteins indicates the critical role this protein has in regulating dendritic outgrowth and branching (39). Although the precise impact of irradiation on these processes is relatively unknown, past work has shown that in immature neurons, overexpression of PSD-95 decreases the proportion of primary dendrites that undergo additional branching, resulting in marked reductions of secondary dendrites (39). These findings are consistent with present observations (Fig. 5), and suggest that radiation-induced overexpression of PSD-95 inhibits dendritic branching and dendritogenesis, leading to reductions in the complexity of the dendritic tree. To analyze the consequences of irradiation on presynaptic sites of the same neurons, the levels of the presynaptic marker synpatophysin were quantified in the DH subfield of the hippocampus. Irradiation was found to induce a persistent and dose-responsive reduction in the level of synaptophysin (Fig. 6), findings that again suggest the capability of irradiation to promote degeneration and compromise neuronal connectivity.

Our data suggest that irradiation has a persistent and adverse impact on the complexity of the dendritic tree, with reductions in dendritic branching, spine density, and alterations in spine morphology and synaptic proteins that are certain to have far-reaching consequences on synaptic plasticity. Past data in the same mouse background (i.e., C57Bl6) has found irradiation to elicit cognitive decrements, albeit at longer postirradiation intervals (9, 10), and data from us and others using different strains of rat have shown irradiation to elicit hippocampal deficits in learning and memory (8, 40, 41). Recent data from us has also shown that low-dose irradiation of the same transgenic mouse strain with charged particles elicits decrements in cognition using a novel object recognition test (42). Based on the foregoing, we anticipate that the changes measured here will be contributory if not causal to radiation-induced cognitive impairment, but given the present dataset this remains speculative. Our study has focused on the neurogenic region of the hippocampus, based on significant past work elucidating the inhibitory effects of irradiation on neurogenesis and the detrimental effects of such exposure on hippocampal learning and memory. Radiation-induced changes found in hippocampal neurons are likely to occur in other neurons throughout the CNS, with some regional variations based on different sensitivities of other neuronal subtypes and their corresponding microenvironments. Our study has provided a detailed analysis of several critical micromorphometric parameters known to impact cognition. Long-lasting reductions in dendritic complexity and spine density, along with alterations in spine morphologies and the composition of synaptic proteins, serve to compromise synaptic plasticity and the functionality of the irradiated brain.

Methods

Animals. Transgenic mice [Jackson Laboratory strain: Tg(Thy1-EGFP)MJrsJ; Stock # 007788] harboring the *Thy1-EGFP* transgene were maintained in accordance with the policies of the University of California Animal Care and Use Committee and the *Guide for the Care and Use of Laboratory Animals*. Mice were housed in ventilated cages, fed a standard pelleted rodent chow, and housed in an environmentally controlled room with a 14:10-h light:dark cycle. Mice were bred (harem) and genotyped to confirm the presence of *Thy1-EGFP* transgene. Male mice positive for the *Thy1-EGFP* transgene were used for all studies.

Radiation Exposure. Mice 2-mo of age were anesthetized and exposed to cranial γ-irradiation (1 or 10 Gy) using a ^{137}Cs irradiator at a dose rate of 2.07 Gy/min, as previously described (8).

Tissue Harvesting. Mice were killed at day 10 or 30 postirradiation by transcardial perfusion with 0.1 M PBS (pH 7.4) followed by 4% (wt/vol) paraformaldehyde. Brains were dissected out, postfixed in 4% (wt/vol) paraformaldehyde for 24 h, washed, and stored in PBS at 4 °C until sectioning. Brains were serially sectioned at 30 or 100 μ on a cryostat (Leica), then cryoprotected at −20 °C.

Immunostaining. To quantify synaptic markers, 30-μm-thick sections were immunostained for PSD-95 or the presynaptic marker synaptophysin. Sections were washed in PBS (pH 7.4), blocked for 30 min in 2% (wt/vol) BSA and 0.1% TritonX 100 (TTX), then incubated for 24 h in a primary antibody mixture containing 1% BSA, 0.1% TTX, mouse anti–PSD-95 (Thermo Scientific; 1:1,000), or mouse antisynaptophysin (Sigma-Aldrich; 1:1,000). Sections were then treated for 1 h with a mixture of goat anti-mouse IgG tagged with Alexa Fluor 594 (1:1,000), rinsed thoroughly in PBS, and sealed in slow fade/antifade mounting medium (Life Technologies).

Confocal Microscopy and Imaging. Homozygous or hemizygous *Thy1-EGFP* mice express EGFP within neurons of the hippocampus and other brain regions, thereby providing a brightly fluorescent signal that greatly facilitates the micromorphometric analyses performed. The exceptional clarity of the fluorescent neurons in these mice provides for an accurate, precise, and rigorous analysis and quantification of the complete dendritic tree. For dendritic analyses, 100-μm-thick hippocampal sections were prepared for confocal imaging. Three sections per animal were used to generate nine *z*-stacks using a Nikon Eclipse TE 2000-U microscope. Images comprising each *z*-stack (1,024 × 1,024 pixels) were acquired at (40×) over the entire dendrite tree at 0.5-μm increments.

Image Processing. For quantification of dendritic parameters, *z*-stacks were reconstructed in 3D from deconvoluted images using the AutoQuantX3 algorithm (MediaCybernetics). Deconvolution combined with 3D reconstruction yields higher spatial resolution images for detailed dendritic tracing and spine classification. For the reconstruction of dendritic filaments and spines, blend intensity *z*-projections were generated using the IMARIS software suite (v7.6, Bitplane) under standardized settings to optimize visualization and analyses.

Neuron Reconstruction. An algorithm for tracing dendritic filaments (IMARIS) was used in autopath mode to reconstruct the entire dendritic tree spanning the series of *z*-stacks (220 × 220 μm^2). This algorithm rebuilds the dendritic tree by tracing individual filaments through the line of maximal fluorescence intensity, starting from the soma of granule cell neurons satisfying predetermined morphologic criteria. Dendritic tracing originated from soma having diameters ranging from 8 to 11 μm, and terminated once dendrite diameters became smaller than 0.6 μm. Once the dendritic tree is reconstructed, the software then reanalyzes dendritic segments for smaller projections or spines. Computer-generated seed points then label individual dendritic spines and following manual verification, quantification of spine number and density is performed. For spines to be included in our analyses, a maximum spine length and minimum spine end diameter were set at 2.5 μm and 0.4 μm, respectively.

Spine Classification. For the quantification of spine morphologies, the total number of spines was counted and classified according to predefined morphologic criteria provided within the IMARIS software suite (i.e., classify spines wizard algorithm). Morphologic parameters for classifying spines are described as follows (43, 44): (*i*) Stubby spine: Diameter of the head is almost equal to the total length of the spine. (*ii*) Long spine: Length of neck is greater than its diameter and the head is clearly distinguishable but has a diameter less than the length of the neck. (*iii*) Mushroom spine: Neck is shorter than it was wide and the diameter of the head is greater than the width of the neck. (*iv*) Filopodia spine: Total spine length is greater than 1 μm with the complete absence of a head.

Quantification of Pre- and Postsynaptic Protein Levels. Analysis of PSD-95 or synaptophysin was performed using the IMARIS spot tool. This feature of the software detects objects (immunostained puncta) within 3D deconvoluted image stacks based on a predefined diameter threshold (1 μm). In a separate channel, the software generates a spot for each puncta detected that can be verified visually for accuracy. To quantify the density of PSD-95 or synaptophysin, the number of PSD-95 or synaptophysin puncta was converted to spots, derived from confocal *z*-stacks taken in 0.5 μm steps at 60×. The "spot quality threshold" and "minimum spot diameter" parameters were manually adjusted to optimize puncta detection and kept constant thereafter for all subsequent analyses.

Statistical Analyses. All morphological data in the present study are derived from four animals per group and presented as the mean ± SEM. The differences in gross dendritic structure (e.g., total dendritic length) and all spine parameters were assessed by ANOVA (GraphPad Prism software, v4.0). *P* values less than 0.05 were considered significant. For multiple comparisons of dendritic and spine parameters, the Bonferroni correction was applied.

ACKNOWLEDGMENTS. We thank Munjal Acharya, Katherine Tran, and Nicole Chmielewski for excellent discussions and technical assistance. This work was supported by the National Institutes of Health National Institute of Neurological Disorders and Stroke Grant R01 NS074388 (to C.L.L.) and by National Aeronautics and Space Administration Grants NNX13AD59G and NNX10AD59G (to C.L.L.).

1. Butler JM, Rapp SR, Shaw EG (2006) Managing the cognitive effects of brain tumor radiation therapy. *Curr Treat Options Oncol* 7(6):517–523.
2. Gorlia T, et al. (2012) New prognostic factors and calculators for outcome prediction in patients with recurrent glioblastoma: A pooled analysis of EORTC Brain Tumour Group phase I and II clinical trials. *Eur J Cancer* 48(8):1176–1184.
3. Meyers CA (2000) Neurocognitive dysfunction in cancer patients. *Oncology (Williston Park)* 14(1):75–79; discussion 79, 81–82, 85.
4. Saury JM, Emanuelson I (2011) Cognitive consequences of the treatment of medulloblastoma among children. *Pediatr Neurol* 44(1):21–30.
5. Barani IJ, et al. (2007) Neural stem cell-preserving external-beam radiotherapy of central nervous system malignancies. *Int J Radiat Oncol Biol Phys* 68(4):978–985.
6. Tofilon PJ, Fike JR (2000) The radioresponse of the central nervous system: A dynamic process. *Radiat Res* 153(4):357–370.
7. Wong CS, Van der Kogel AJ (2004) Mechanisms of radiation injury to the central nervous system: Implications for neuroprotection. *Mol Interv* 4(5):273–284.
8. Acharya MM, et al. (2009) Rescue of radiation-induced cognitive impairment through cranial transplantation of human embryonic stem cells. *Proc Natl Acad Sci USA* 106(45): 19150–19155.
9. Raber J, et al. (2004) Radiation-induced cognitive impairments are associated with changes in indicators of hippocampal neurogenesis. *Radiat Res* 162(1):39–47.
10. Rola R, et al. (2004) Radiation-induced impairment of hippocampal neurogenesis is associated with cognitive deficits in young mice. *Exp Neurol* 188(2):316–330.
11. Fike JR, Rosi S, Limoli CL (2009) Neural precursor cells and central nervous system radiation sensitivity. *Semin Radiat Oncol* 19(2):122–132.
12. Mizumatsu S, et al. (2003) Extreme sensitivity of adult neurogenesis to low doses of X-irradiation. *Cancer Res* 63(14):4021–4027.
13. van Praag H, et al. (2002) Functional neurogenesis in the adult hippocampus. *Nature* 415(6875):1030–1034.
14. Huttenlocher PR (1991) Dendritic and synaptic pathology in mental retardation. *Pediatr Neurol* 7(2):79–85.
15. Kolb B, Whishaw IQ (1998) Brain plasticity and behavior. *Annu Rev Psychol* 49: 43–64.
16. Tronel S, et al. (2010) Spatial learning sculpts the dendritic arbor of adult-born hippocampal neurons. *Proc Natl Acad Sci USA* 107(17):7963–7968.
17. Nishimura M, Gu X, Swann JW (2011) Seizures in early life suppress hippocampal dendrite growth while impairing spatial learning. *Neurobiol Dis* 44(2):205–214.
18. Bremner JD, Krystal JH, Southwick SM, Charney DS (1995) Functional neuroanatomical correlates of the effects of stress on memory. *J Trauma Stress* 8(4):527–553.
19. Terry RD, Peck A, DeTeresa R, Schechter R, Horoupian DS (1981) Some morphometric aspects of the brain in senile dementia of the Alzheimer type. *Ann Neurol* 10(2):184–192.
20. Kaufmann WE, Moser HW (2000) Dendritic anomalies in disorders associated with mental retardation. *Cereb Cortex* 10(10):981–991.
21. Takashima S, Iida K, Mito T, Arima M (1994) Dendritic and histochemical development and ageing in patients with Down's syndrome. *J Intellect Disabil Res* 38 (Pt 3):265–273.
22. Armstrong DD, Dunn K, Antalffy B (1998) Decreased dendritic branching in frontal, motor and limbic cortex in Rett syndrome compared with trisomy 21. *J Neuropathol Exp Neurol* 57(11):1013–1017.
23. van Spronsen M, Hoogenraad CC (2010) Synapse pathology in psychiatric and neurologic disease. *Curr Neurol Neurosci Rep* 10(3):207–214.
24. Pfeiffer BE, Huber KM (2009) The state of synapses in fragile X syndrome. *Neuroscientist* 15(5):549–567.
25. Selkoe DJ (2002) Alzheimer's disease is a synaptic failure. *Science* 298(5594): 789–791.
26. Yuste R, Bonhoeffer T (2001) Morphological changes in dendritic spines associated with long-term synaptic plasticity. *Annu Rev Neurosci* 24:1071–1089.
27. Yuste R, Bonhoeffer T (2004) Genesis of dendritic spines: Insights from ultrastructural and imaging studies. *Nat Rev Neurosci* 5(1):24–34.
28. Blanpied TA, Ehlers MD (2004) Microanatomy of dendritic spines: Emerging principles of synaptic pathology in psychiatric and neurological disease. *Biol Psychiatry* 55(12): 1121–1127.
29. Dickstein DL, Weaver CM, Luebke JI, Hof PR (2012) Dendritic spine changes associated with normal aging. *Neuroscience*, 10.1016/j.neuroscience.2012.09.077.
30. Yoshihara Y, De Roo M, Muller D (2009) Dendritic spine formation and stabilization. *Curr Opin Neurobiol* 19(2):146–153.
31. Matsuzaki M, Honkura N, Ellis-Davies GC, Kasai H (2004) Structural basis of long-term potentiation in single dendritic spines. *Nature* 429(6993):761–766.
32. Chen Y, et al. (2010) Correlated memory defects and hippocampal dendritic spine loss after acute stress involve corticotropin-releasing hormone signaling. *Proc Natl Acad Sci USA* 107(29):13123–13128.
33. Rosi S, et al. (2008) Cranial irradiation alters the behaviorally induced immediate-early gene arc (activity-regulated cytoskeleton-associated protein). *Cancer Res* 68(23): 9763–9770.
34. Greene-Schloesser D, Robbins ME (2012) Radiation-induced cognitive impairment—From bench to bedside. *Neuro-oncol* 14(Suppl 4):iv37–iv44.
35. Greene-Schloesser D, et al. (2012) Radiation-induced brain injury: A review. *Front Oncol* 2(73):1–18.
36. Zou Y, et al. (2012) Extracellular superoxide dismutase is important for hippocampal neurogenesis and preservation of cognitive functions after irradiation. *Proc Natl Acad Sci USA* 109(52):21522–21527.
37. Chakraborti A, Allen A, Allen B, Rosi S, Fike JR (2012) Cranial irradiation alters dendritic spine density and morphology in the hippocampus. *PLoS ONE* 7(7):e40844.
38. Woods GF, Oh WC, Boudewyn LC, Mikula SK, Zito K (2011) Loss of PSD-95 enrichment is not a prerequisite for spine retraction. *J Neurosci* 31(34):12129–12138.
39. Charych EI, et al. (2006) Activity-independent regulation of dendrite patterning by postsynaptic density protein PSD-95. *J Neurosci* 26(40):10164–10176.
40. Acharya MM, et al. (2011) Human neural stem cell transplantation ameliorates radiation-induced cognitive dysfunction. *Cancer Res* 71(14):4834–4845.
41. Winocur G, Wojtowicz JM, Sekeres M, Snyder JS, Wang S (2006) Inhibition of neurogenesis interferes with hippocampus-dependent memory function. *Hippocampus* 16(3):296–304.
42. Tseng BP, et al. (2013) Functional consequences of radiation-induced oxidative stress in cultured neural stem cells and the brain exposed to charged particle irradiation. *Antioxid Redox Signal*, in press.
43. Harris KM, Jensen FE, Tsao B (1992) Three-dimensional structure of dendritic spines and synapses in rat hippocampus (CA1) at postnatal day 15 and adult ages: Implications for the maturation of synaptic physiology and long-term potentiation. *J Neurosci* 12(7):2685–2705.
44. Rodriguez A, Ehlenberger DB, Dickstein DL, Hof PR, Wearne SL (2008) Automated three-dimensional detection and shape classification of dendritic spines from fluorescence microscopy images. *PLoS ONE* 3(4):e1997.